MOLECULAR AND CELLULAR BIOLOGY, Jan. 2007, p. 20–30 Vol. 27, No. 1
0270-7306/07/$08.00+0 doi:10.1128/MCB.00824-06

AID Associates with Single-Stranded DNA with High Affinity and a Long Complex Half-Life in a Sequence-Independent Manner▽

Mani Larijani,[1] Alexander P. Petrov,[2] Oxana Kolenchenko,[1] Maribel Berru,[1] Sergey N. Krylov,[2] and Alberto Martin[1]*

Department of Immunology, University of Toronto, Medical Sciences Building, Toronto, Canada M5S 1A8,[1] *and Department of Chemistry, York University, Toronto, Ontario, Canada M3J 1P3*[2]

Received 9 May 2006/Returned for modification 29 June 2006/Accepted 6 October 2006

Activation-induced cytidine deaminase (AID) initiates secondary antibody diversification processes by deaminating cytidines on single-stranded DNA. AID preferentially mutates cytidines preceded by W(A/T)R(A/G) dinucleotides, a sequence specificity that is evolutionarily conserved from bony fish to humans. To uncover the biochemical mechanism of AID, we compared the catalytic and binding kinetics of AID on WRC (a hot-spot motif, where W equals A or T and R equals A or G) and non-WRC motifs. We show that although purified AID preferentially deaminates WRC over non-WRC motifs to the same degree observed in vivo, it exhibits similar binding affinities to either motif, indicating that its sequence specificity is not due to preferential binding of WRC motifs. AID preferentially deaminates bubble substrates of five to seven nucleotides rather than larger bubbles and preferentially binds to bubble-type rather than to single-stranded DNA substrates, suggesting that the natural targets of AID are either transcription bubbles or stem-loop structures. Importantly, AID displays remarkably high affinity for single-stranded DNA as indicated by the low dissociation constants and long half-life of complex dissociation that are typical of transcription factors and single-stranded DNA binding protein. These findings suggest that AID may persist on immunoglobulin and other target sequences after deamination, possibly acting as a scaffolding protein to recruit other factors.

Activation-induced cytidine deaminase (AID) is the B-cell-specific enzyme responsible for the conversion of cytidine to uridine, the initiating event in somatic hypermutation (SHM) and class switch recombination (CSR) of antibody genes (20, 22, 26, 29). This initial lesion can either be replicated, producing a transition mutation, or be engaged by the base excision (i.e., UNG) (34) or mismatch repair pathways (i.e., MSH2) (21, 33, 52), resulting in transversion mutations or A-T mutations, respectively. Cytidine deamination by AID also leads to the generation of double-stranded lesions in the switch regions of antibody genes, leading to CSR (9, 22, 42, 43).

While necessary for SHM and CSR, AID-induced lesions have been shown to cause chromosomal translocations contributing to lymphoma (13, 36, 37). Because of this inherently dangerous property of AID, it is likely that the activity of AID is controlled at different levels to focus it on immunoglobulin genes, such as through protein kinase A phosphorylation (2, 27) or the interaction with cofactors, such as replication protein A (RPA) (7). At the target DNA level, high levels of transcription have been shown to be necessary but not sufficient for AID activity (1, 22, 23, 28, 38). Since AID is able to deaminate cytidines only on single-stranded DNA (ssDNA) (6, 8, 10, 17, 18, 25, 47), it is likely that the requirement for transcription reflects the generation of single-stranded regions by transcription bubbles (8, 22) or the generation of G4 DNA structures (11, 12).

Even prior to the discovery of AID, it was noted that SHM occurs more frequently in cytidines that are preceded by a W(A/T)R(A/G) motif (40). As a result, this motif has been termed a hot-spot motif. The increased mutability of WRC (where W equals A or T and R equals A or G) motifs in SHM is conserved from mice and humans (39, 44) to zebrafish and catfish (50). Purified AID preferentially deaminates WRC motifs on a stretch of ssDNA in vitro, indicating that WRC sequence specificity is an inherent AID trait and independent of any cofactors (17, 18, 31, 54). Findings that CSR breakpoints occur at or near AGCT motifs (15, 55), which are WRC motifs on both strands, argues that the WRC specificity of AID is a significant regulator of its activity.

Although AID deaminates cytidines in vitro, the molecular mechanisms of target DNA capture and WRC specificity are unknown. Determination of the enzymatic properties of AID at the molecular level is, hence, necessary to understand the catalytic mechanism of AID. In this report, we evaluated the enzymatic as well as complex formation properties of purified AID on partially single-stranded "bubble" substrates as well as fully ssDNA substrates to determine the K_m, K_d, and other properties of substrate binding and catalysis by AID.

MATERIALS AND METHODS

AID purification. For glutathione transferase (GST)-AID, an EcoRI fragment containing human AID was cloned into pGEX-5x-3 GST (Amersham), expressed in *Escherichia coli* BL21(DE3) and induced by the addition of 1 mM IPTG (isopropyl-β-D-thiogalactopyranoside) to a log-phase culture, followed by incubation for 16 h at 16°C. Cells were lysed in a French pressure cell press (Thermospectronic), and the supernatant was applied to a column of glutathione-Sepharose high-performance beads (Amersham) as per the manufacturer's recommendations. GST-AID was purified on glutathione-Sepharose beads (Amersham) as per the manufacturer's recommendations. GST-AID of ~80% purity was dialyzed in 20 mM Tris-Cl, pH 7.5, 100 mM NaCl, 1 mM dithiothreitol (DTT). The empty pGEX-5x-3 vector was used to purify GST as a control for

* Corresponding author. Mailing address: Department of Immunology, University of Toronto, Medical Sciences Bldg. 5265, Toronto, Canada M5S 1A8. Phone: (416) 978-4235. Fax: (416) 978-1938. E-mail: alberto.martin@utoronto.ca.

▽ Published ahead of print on 23 October 2006.

activity assays and electrophoretic mobility shift assay (EMSA). The purification of His-AID has been previously described (14). Although His-AID was purified to ~90% purity, bacteria harboring the empty pRSET/C vector were induced and used in parallel purification processes to generate a control for activity and binding assays.

Substrate preparation. Sequences of single-stranded and bubble substrates are shown in Fig. 1. The bubble substrates are similar to those previously described (47) only differing from each other in the dinucleotide before the target C, constituting hot or cold spots. A total of 5 pmol of the bottom strand (Fig. 1) was 5′ labeled with [γ-^{32}P]dATP using polynucleotide kinase (NEB) and purified through mini-Quick spin DNA columns (Roche). For the labeled substrates, a 2:1 ratio of top:bottom strand was annealed in a volume of 50 to 100 μl. Unlabeled competitor bubbles were annealed at a 1:1 ratio.

Deamination assay. The assay was a variation of assays described previously (47, 54). Briefly, 0.1 to 500 fmol of labeled substrate was incubated with 0.3 to 0.9 μg of GST-AID or His-AID for 90 min at 37°C in 50 mM Tris, pH 7.5, 100 mM NaCl, and 2 μM MgCl in a volume of 10 μl. AID was then deactivated for 15 min at 75°C. The volume was then increased to 20 μl and 1 unit of uracil DNA glycosylase and buffer (NEB) were added for a 90-min incubation period of 37°C in order to excise the uracil generated by the deamination of the target cytidine. Finally, 2.2 μl of 1 M NaOH was added, and the samples were heated to 95°C for 8 min to cleave the alkali-labile abasic site. Samples were electrophoresed at room temperature on a 20% denaturing acrylamide gel with a running buffer of 1× TBE (Tris-borate-EDTA) at 300 V for 3 h and visualized using a PhosphorImager (Molecular Dynamics). Quantitation was done using ImageQuant software, version 5.0 (Molecular Dynamics).

EMSA. Indicated amounts (from 0.15 to 50 fmol [see the legend to Fig. 4]) of labeled substrate were incubated with 0.3 to 1 μg of GST-AID or His-AID in a buffer containing 50 mM Tris, pH 7.5, 2.0 μM MgCl, 50 mM NaCl, and 1 mM DTT in a final volume of 10 μl at 25°C for 45 min. GST, which was purified in parallel to GST-AID, was used as a control in all lanes which did not contain GST-AID in order to demonstrate specific complex formation. A similar empty-vector control was used to ensure the specificity of the shifted bands obtained with His-AID. Samples were then either immediately loaded on the gel or UV cross-linked (Stratagene) on ice at a distance of 2 cm from the UV source with 100 mJ and an irradiation time of 50 s. Samples were electrophoresed at 4°C on an 8% native gel (0.5× TBE, 6% glycerol, 8% acrylamide:bisacrylamide [19:1]) with a running buffer of 0.5×TBE at 300 V for 3 h. Gels were dried and visualized using a PhosphorImager (Molecular Dynamics). All quantitation was done using ImageQuant software, version 5.0 (Molecular Dynamics). Data were plotted as bound and free fractions of the substrate. For the determination of approximate half-saturation values, Sigmaplot version 5.0 was used to fit the data to the following equation derived from the law of mass action: $[\text{Bound}] = ([\text{Bound}_{max}] \times [\text{free}])/(K_d + [\text{free}])$, where $[\text{Bound}_{max}]$ represents the maximum amount of bound substrate at saturation and is assumed to equal the molar amount of total active AID (32, 49). Because AID and substrates do not dissociate in EMSAs involving UV cross-linking, the Bound_{max} in EMSAs involving UV cross-linking (see Fig. 4 and 5), which was ~4 fmol, indicates that ~4 fmol of active AID existed in the preparations, assuming a 1:1 AID:substrate stoichiometry. That is, substrate concentrations beyond 4 fmol did not generate any additional AID:DNA complexes, indicating that all active AID was bound at this concentration. As 10 pmol of AID was added for each reaction, this indicates a ratio of 1:5,000 active AID:total AID in all enzymatic and binding assays analyzed. This ratio represents a lower limit estimate as maximal cross-linking efficiency and 1:1 stoichiometry were assumed.

NECEEM. For a detailed description of a nonequilibrium capillary electrophoresis (NECEEM) assay, see Berezovski and Krylov (3). Briefly, 1 pmol of fluorescent oligonucleotide was incubated with 1.5 μg of GST-AID in 50 mM Tris-HCl (pH 7.5), 2.0 μM $MgCl_2$, 50 mM NaCl, and 1 mM DTT at 37°C for 45 min. Electrophoresis was carried out with a P/ACE MDQ apparatus (Beckman Coulter, Mississauga, Ontario, Canada) equipped with a fluorescence detector and a 488-nm line of an Ar-ion laser to excite fluorescence. A 50-cm-long uncoated fused silica capillary with an inner diameter of 75 μm and an outer diameter of 360 μm was used. Capillary temperature was maintained at 20°C. Inlet and outlet reservoirs and the capillary were prefilled with the run buffer. A plug of the AID-DNA equilibrium mixture was injected into the capillary by a pressure pulse of 0.5 lb/in^2 for 5 s; the length and volume of the injected equilibrium mixture were 7 mm and 30 nl, respectively. The ends of the capillary were inserted in the inlet and outlet reservoirs, and the electric field was applied. Protein-DNA complex, DNA dissociated from the complex during separation, and free DNA were detected. Fast dissociation was monitored to obtain both the rate constant, k_{off}, and the equilibrium constant, K_d, of complex dissociation. The constants are calculated using areas and migration times of peaks from an electropherogram: $k_{off} = \ln(A_{complex} + A_{dissociation})/A_{complex}/t_{complex}$ and $K_d = ([P]_0(1 + A_{DNA}/A_{complex}) - [DNA]_0)/1 + A_{complex}/A_{DNA}$. $A_{complex}$, $A_{dissociation}$, and A_{DNA} are areas corresponding to the intact complex, DNA dissociated from

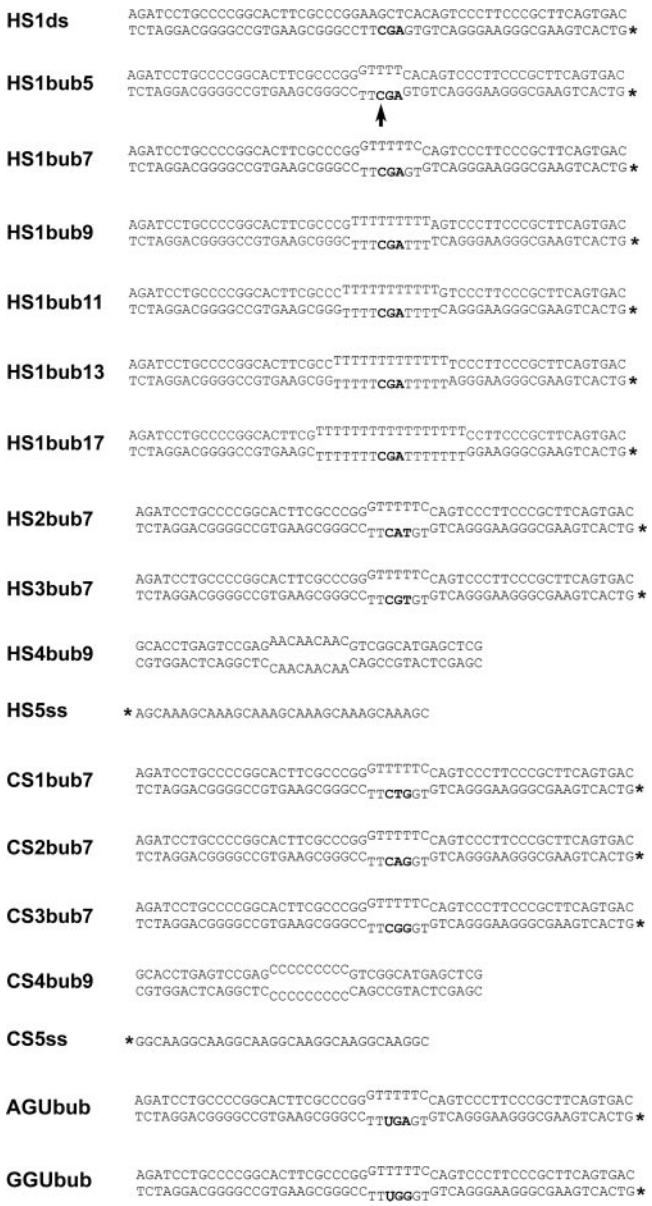

FIG. 1. Sequences of the DNA substrates used in binding and activity assays. All substrates used in activity assays contain a single cytidine within the bubble and differ in the dinucleotide immediately upstream of the target cytidine constituting either WRC motifs (hot spots) or non-WRC motifs (cold spots). *, radioactively labeled strand; HS, bubble containing a hot-spot motif; CS, bubble containing a cold-spot motif. The last number of each substrate indicates the size of the single-stranded bubble portion. The position of the target cytidine within the bubble is indicated by an arrow for HS1bub5. HS4bub9 and CS4bub9 contain repeats of the hot-spot sequence AAC and the cold-spot CCC, respectively, and were used as unlabeled competitors in activity assays. The single-stranded substrates HS5ss and CS5ss containing tandem repeats of hot or cold spots were used in EMSAs as well as NECEEM assays to measure AID binding. AGUbub and GGUbub are analogous to HS1bub7 and CS3bub7 except for the substitution of uridine for cytidine.

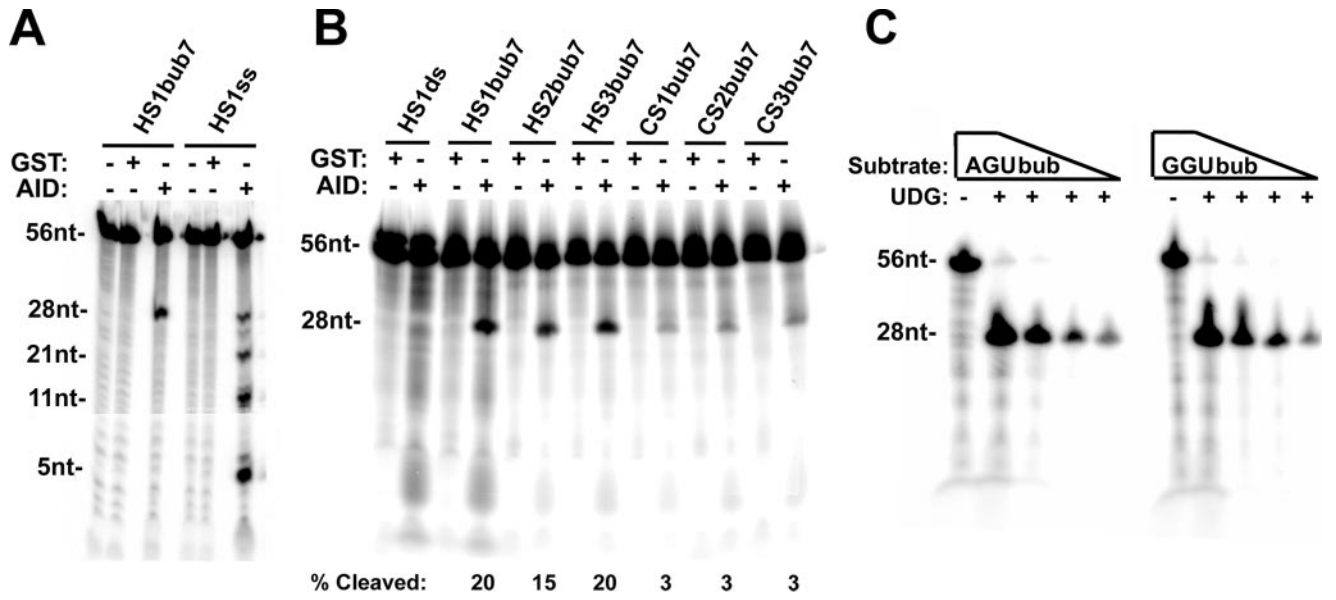

FIG. 2. Deamination analysis on hot- and cold-spot bubbles. (A) Deamination assay showing GST-AID activity on a bubble substrate (HS1bub7) as well as the single-stranded HS1ss (the radioactively labeled strand of HS1bub7). As indicated at top, GST was purified in parallel with GST-AID and used as a control for the specific activity of AID. The top band represents the 56-nucleotide labeled strand and the lower band represents the 28-nucleotide product of deamination due to alkaline cleavage at the target C in the bubble. UDG was added to all reactions. (B) Deamination assay comparing AID activities on three hot-spot bubbles (HS1bub7, HS2bub7, and HS3bub7) and three cold-spot bubbles (CS1bub7, CS2bub7, and CS3bub7). HS1ds was used as a control for the single-stranded DNA activity of AID. The band intensities were quantitated, and the amount of cleaved product resulting from deamination as a percentage of the entire labeled DNA in each lane is shown below each substrate. (C) As a control to ensure that the UDG step of the activity reaction does not discriminate between WRU and non-WRU motifs, UDG (without AID) was incubated with serial dilutions of AGUbub or GGUbub substrates which were designed to be analogous to HS1bub7 and CS3bub7 but with the target cytidine on the labeled strand replaced by uridine. nt, nucleotide.

the complex, and free DNA, respectively. $[P]_0$ and $[DNA]_0$ are concentrations of active enzyme and DNA, respectively.

Size exclusion chromatography of AID. GST-AID was purified as described above and dialyzed in a buffer containing 50 mM Tris, pH 8.0, 50 mM NaCl, and 5 mM EDTA. As GST-AID is active in this buffer, it was also used as the column equilibration and run buffer. GST-AID was concentrated to a volume of 2 ml using a Vivaspin-2 column (Vivascience) with a 10,000-molecular-weight limit and loaded on a Hi-Load 16/60 Superdex 200 preparative-grade column. An automated AKTA fast protein liquid chromatography (FPLC) machine (model UPC900; Amersham) and Unicorn 5 software were used for this analysis. Column calibration was performed using standard proteins of known sizes and dextran for accurate determination of the column's void volume. Four-milliliter fractions were collected and concentrated to a volume of 150 μl using Vivaspin-2 columns. Deamination assays were set up by incubating 1 μl of HS1bub7 substrate (20 fmol) with 8 μl of each concentrated fraction and 1 μl of uracil DNA glycoslyase (UDG; 1 unit) (NEB). ImageQuant, version 5.0 (Molecular Dynamics), was used for quantitation of the results. The amount of GST-AID in each fraction was calculated from the UV absorption values during elution from the column and used along with the amount of substrate and incubation time to obtain the specific activity of each fraction.

RESULTS

Quantitative measurement of AID deamination. AID preferentially deaminates cytidines within WRC hot-spot motifs on long stretches of ssDNA (17, 18, 31). However, accurate comparison of AID activities on different hot-spot and cold-spot sequence motifs could not be made due to the possibility that WRC and non-WRC sequences influence AID activity on each other and the suggested processivity of the AID enzyme (31). Here, we established an in vitro experimental system in which the activity of in vitro-purified GST or His-tagged AID (i.e., GST-AID or His-AID) could be quantitatively evaluated on individual substrates bearing single hot or cold spots. In this assay, the uridine produced by AID is removed by UDG, resulting in an abasic site which is the subject of alkaline cleavage. Figure 1 shows the substrates used in these assays. Each bubble substrate containing a WRC (hot spot) or non-WRC (cold spot) motif has a 5- to 17-nucleotide bubble, and only the dinucleotide preceding the target cytidine is varied among substrates, thus creating hot-spot or cold-spot bubbles (i.e., HSbub or CSbub). Figure 2A shows the activity of GST-AID on a bubble-type substrate (HS1bub7) and on the labeled (bottom) strand of the same substrate (HS1ss). As expected, GST-AID deaminated multiple cytidines on the single-stranded substrate, giving rise to multiple alkaline cleavage products. No cleavage product was observed in control GST-treated preparations (Fig. 2A), and assays using in vitro-purified mutants of GST-AID that were catalytically dead resulted in no product bands (data not shown). In contrast, the only apparent product on the bubble substrate corresponds in size to the target cytidine in the bubble (Fig. 2A). This result confirms the ssDNA activity of AID and, more importantly, validates the structure of the bubble substrate.

We then compared GST-AID activities on six different hot- and cold-spot bubbles as shown in Fig. 2B. While 15 to 20% of the hot-spot bubble substrates were deaminated, 3% of the cold-spot bubbles were deaminated. As expected, no alkaline cleavage product was obtained from the fully double-stranded HS1ds substrate. This five- to eightfold preference of GST-AID for hot spots was also observed when His-AID was used in the UDG assay (see below) and is similar to that observed in

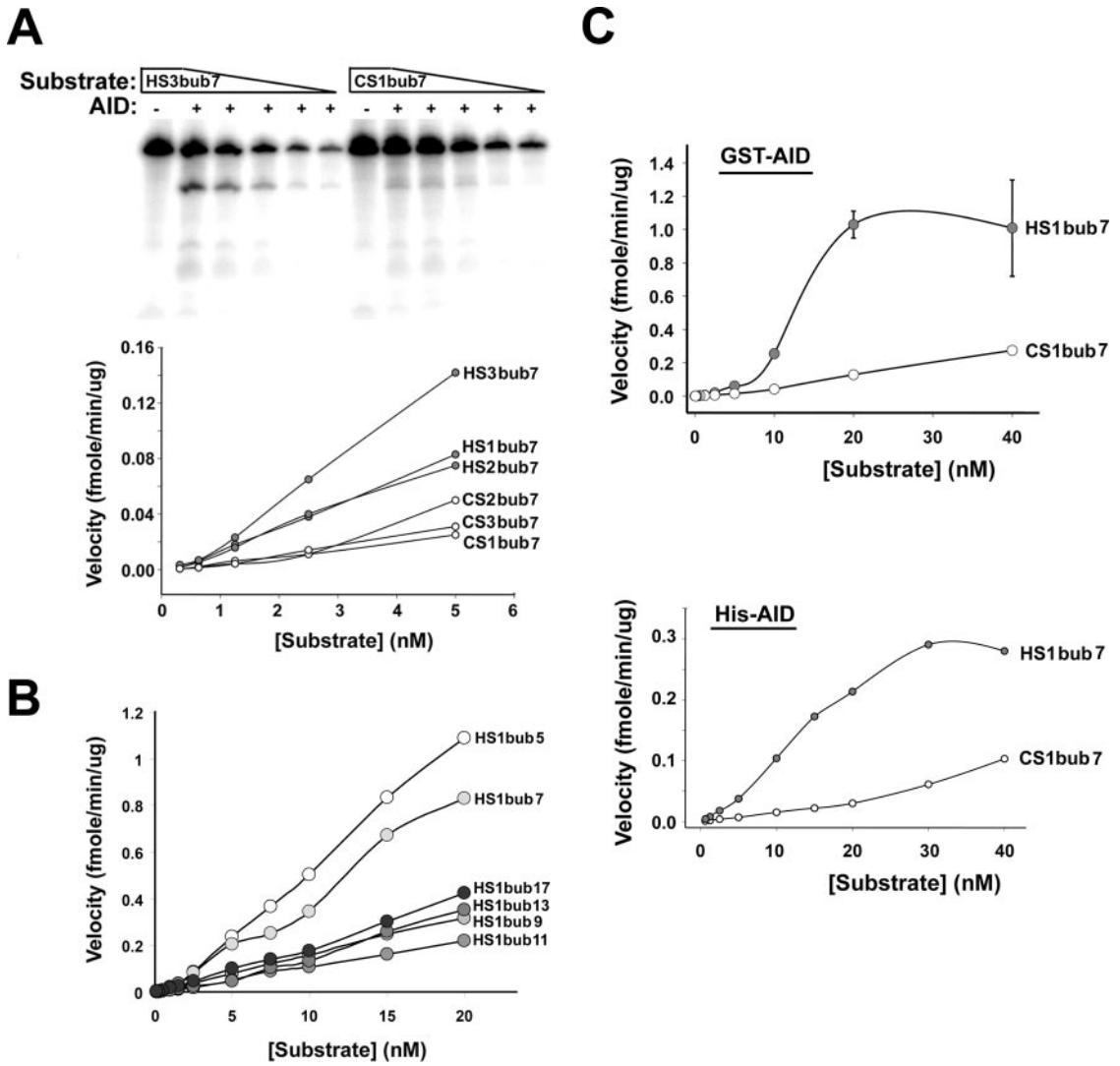

FIG. 3. Deamination kinetics on hot- and cold-spot bubbles. (A) Representative deamination assay showing the activity of GST-AID on serial dilutions of a hot-spot and a cold-spot bubble. Assays were performed on the indicated hot-spot bubbles and cold-spot bubbles using constant concentrations of GST (−) or GST-AID (+) and twofold serial dilutions of the substrate starting with 5 nM. The product and substrate bands were quantitated and used together with the incubation time and the amount of AID to calculate the reaction velocity at each substrate concentration (graph). Velocity is defined as the amount of deaminated product generated by a given amount of AID in a unit of time and plotted against substrate concentration. (B) Deamination kinetics showing the activity of GST-AID on dilutions (starting with 20 nM) of hot-spot substrates with the same WRC motif (AGC) located within different bubble sizes ranging from 5 (HS1bub5) to 17 (HS1bub17) nucleotides. (C) Reaction velocity plotted against substrate concentration carried out over a 1,000-fold range of substrate concentration (starting with 40 nM) on HS1bub7 and CS1bub7 for GST-AID and His-AID.

hypermutating Ramos cells (56). To ensure that the production of the cleaved product was not due to preferential activity of UDG on WRU motifs, UDG was incubated with AGU and GGU bubble (AGUbub and GGUbub, respectively) substrates. These substrates, as shown in Fig. 1, are analogous to HS1bub7 and CS3bub7, respectively, but with the target cytidine replaced by uridine. As shown in Fig. 2C, there was no difference in the generation of the cleaved product between AGUbub and GGUbub, and the UDG incubation conditions were sufficient to completely convert the substrate into product. Thus, the difference in the levels of the cleaved product between the hot-spot and cold-spot bubbles is solely attributable to the action of AID.

Deamination kinetics on hot- and cold-spot bubbles. After performing time course and GST-AID dilution experiments to ensure that we were working within the linear range for the activity assay (data not shown), we compared the appearances of the deaminated product as a function of substrate concentration for all six hot- and cold-spot substrates. A representative assay is shown in Fig. 3A (top). The velocity of product formation was determined by calculating the amount of product formed in a unit of time by a given amount of GST-AID and plotted against substrate concentration. As shown in Fig. 3A (graph), the velocity of product formation was appreciably higher on all hot-spot bubbles than on the cold-spot bubbles. A similar result was observed when His-AID was used in the

deamination assays (Fig. 3C, lower graph). Consistent with our previous observations with His-AID (17, 18), we found that preincubation of GST-AID with RNase A did not change the kinetic properties of AID (data not shown). This is in contrast to AID expressed in insect cells that require preincubation with RNase to be active (6, 54).

We sought to examine whether the relative size of the bubble itself can influence the activity of AID. Thus, we compared the activities of GST-AID on substrates bearing the same WRC motif (AGC) but in the context of bubble sizes ranging from 5 to 17 nucleotides long. These substrates are illustrated in Fig. 1 (HS1bub5 to HS1bub17), and the results of the deamination assay are shown in Fig. 3B. Surprisingly, GST-AID was more active on 5- and 7-nucleotide bubbles than on their longer counterparts which more closely represent the size of in vivo transcription bubbles. The significance of this finding is discussed below.

At the point of maximal difference, the velocity of deamination of HS1bub7 by GST-AID and His-AID was ca. eightfold higher than for CS1bub7 (Fig. 3C). The K_m of GST-AID and His-AID for HS1bub7 was between 10 and 15 nM. It was not possible to estimate the K_m for the cold-spot bubble (i.e., CS1bub7) since substrate saturation kinetics was not observed. However, as the velocity continues to increase beyond the highest substrate concentration tested, the K_m is likely to be severalfold higher for CS1bub7 than for HS1bub7. By estimating the fraction of active GST-AID in our preparations (see next section), we were able to calculate the catalytic efficiency of GST-AID. At V_{max}, the k_{cat} for GST-AID was calculated to be 0.0042 s^{-1} (i.e., 1.0 fmol of substrate/60 s/4 fmol of active GST-AID) or 1 deamination event every 4 min for each AID protein. Thus, AID displays a very low catalytic efficiency relative to other enzymes (see Discussion for further elaboration).

AID complex formation on hot- and cold-spot bubbles. We employed EMSAs to measure the binding kinetics of GST-AID to the same hot- and cold-spot bubbles used in the activity assays. To initially test whether GST-AID binds to single- or double-stranded DNA, we compared the levels of binding to the HS1bub7 and the double-stranded HS1ds substrate, which is identical to HS1bub7 but lacks the mismatched bubble region (Fig. 1). As shown in Fig. 4A (− lanes), purified GST did not form complexes with HS1ds or HS1bub7. Complex formation between AID and HS1ds was negligible (Fig. 4A, middle gel), as has been previously shown (10). In contrast, two shifted bands (likely representing complexes with different stoichiometries) resulted from the incubation of AID with the bubble substrate (Fig. 4A, left gel). This result shows that AID binds to the single-stranded bubble region of bubble substrates. The right gel in Fig. 4A shows an EMSA carried out on HS1bub7 using GST-AID and His-AID in parallel. Importantly, multiple complexes are also apparent with His-AID, indicating that the formation of multiple complexes differing in mobility is a characteristic of AID rather than an artifact of its purification tag.

To obtain approximate dissociation constant (K_d) values reflective of half-saturation of AID with hot-spot and cold-spot bubbles, complex formation was measured by EMSA over a nearly 200-fold range of substrate concentrations. EMSAs were performed with and without UV cross-linking. In the absence of UV cross-linking, complexes can dissociate during electrophoresis, which might affect the calculated K_d since the equilibrium can be affected during electrophoresis. In contrast, with UV cross-linking of AID to substrates, dissociation will not occur during electrophoresis, and thus the data would represent a snapshot at a specific point in time of the total interaction between AID and the substrate. So that UV cross-linking does not introduce biases in the measured K_d, the time of irradiation should be shorter than characteristic times of complex formation ($[DNA]^{-1} k_{on}^{-1}$) and complex dissociation (k_{off}^{-1}). The 50-s irradiation time used here satisfied both conditions (see below). The EMSA experiment with cross-linking also allowed us to estimate the concentration of the active GST-AID in the sample (see Materials and Methods). This value (i.e., ~4 fmol of active AID used in both the EMSA and kinetic assays) was used to calculate the k_{cat} in the previous section.

Representative EMSA results of GST-AID binding to a hot- and cold-spot bubble are shown in Fig. 4B and C, respectively. The relative amounts of free DNA and bound DNA were determined at each input DNA concentration and plotted. The apparent dissociation constant (K_d) was derived using a nonlinear regression analysis of the data (see Materials and Methods). As expected, higher overall levels of bound complex were observed with UV cross-linking. Nevertheless, the K_d values with or without UV cross-linking were similar between HS3bub7 and CS3bub7 and ranged between 0.3 and 1.2 nM (Fig. 4B and C). GST-AID also bound to HS1bub7 with a similar K_d of 0.3 nM (Table 1). To assess whether these data were influenced by the GST tag, we also performed EMSA analysis using His-AID on HS1bub7 and CS1bub7. As with GST-AID, there was no significant difference between the binding affinities of His-AID to a hot- or cold-spot bubble (Table 1). These data suggest that AID binds ssDNA regardless of sequence. To confirm this, we performed EMSA using GST-AID and AGUbub, which is analogous to HS1bub7 with the cytidine replaced by uridine. Indeed, GST-AID formed stable complexes with AGUbub, indicating that a cytidine is not required for AID binding (data not shown).

Using the same EMSA analysis, we also determined the binding affinities of GST-AID to HS1bub5 and HS1bub11. As HS1bub5 and HS1bub7 were more efficient substrates for AID deamination than HS1bub11, we assessed whether this was due to differences in binding affinities. As shown in Table 1, GST-AID bound to HS1bub5, HS1bub7, and HS1bub11 with similar K_d values (i.e., 1.1, 0.3, and 0.5 nM, respectively), suggesting that the preferential activity of AID to small bubble substrates was not due to preferential binding. In conclusion, dissociation constants for all bubble substrates tested were in the 0.3 to 2.0 nM range, indicating that AID binds these bubble substrates with very high affinities regardless of size and sequence.

The high binding affinities of AID to bubble substrates suggests that AID forms stable complexes with long half-lives. To determine the complex half-life, GST-AID was incubated with radioactively labeled HS1bub7, allowing sufficient time for complex formation, followed by the addition of 500-fold excess unlabeled HS1bub7 for various lengths of time before UV cross-linking. Since the vast excess of unlabeled competitor prevents reassociation of AID to the radioactive substrate once an AID-DNA complex has dissociated, this method allows for a measurement of the rate of decay of the complex. Based on

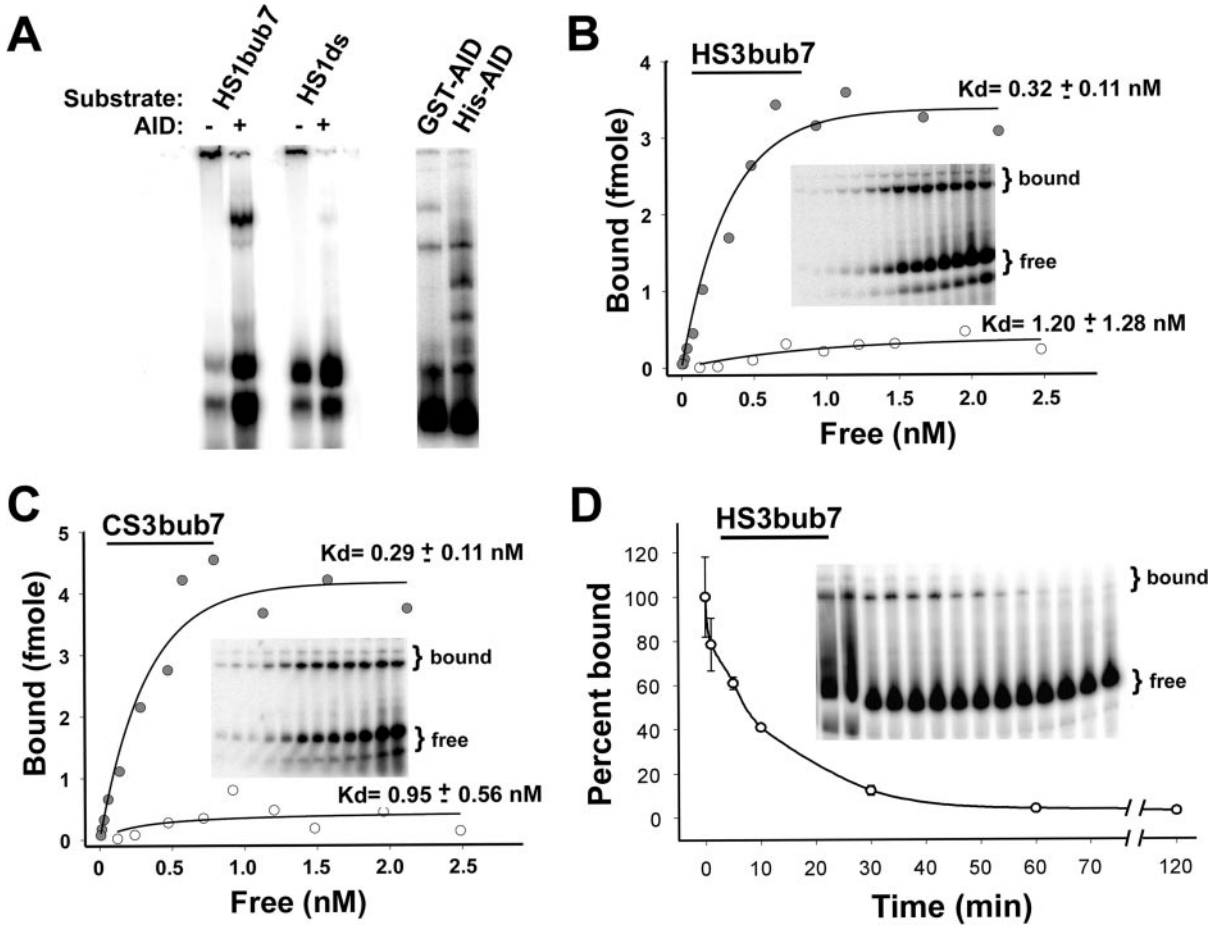

FIG. 4. EMSA measuring AID binding to bubble substrates. (A) EMSA with GST (−) or GST-AID (+) on HS1bub7 and HS1ds demonstrating the dependence of complex formation on the presence of a bubble structure (left and middle gels). EMSA comparing GST-AID and His-AID binding levels on HS1bub7 (right gel). (B) Representative EMSA experiment on a hot-spot bubble (HS3bub7) substrate. EMSA reactions were carried out in the presence of increasing amounts of the bubble substrate over a range of 0.15 to 50 fmol and electrophoresed in native conditions. In order to obtain half-saturation (K_d) values of interaction, the fraction of shifted substrate was quantitated for each lane and a bound-versus-free plot was generated. Filled circles represent results from an EMSA with UV cross-linking (the gel is shown) while empty circles represent results from an EMSA without UV cross-linking (gel not shown). (C) The same experiment as shown in panel B, except that CS3bub7 was used as the substrate in the EMSA experiment. (D) EMSA measuring the complex half-life of GST-AID bound to HS1bub7. Binding reactions were set up using 20 fmol of HS1bub7 as substrate and incubated for 45 min to allow for complex formation. A 500-fold excess (10 pmol) of unlabeled HS1bub7 was then added to the binding mixture, followed by incubation for various lengths of time as indicated on the *x* axis from 0 to 120 min prior to UV cross-linking of the reaction. The start times of the EMSA reactions were staggered such that all time points ended concurrently. Each time point was done in duplicate starting with 0, 5, 10, 30, 60, and 120 min of incubation after the addition of unlabeled HS1bub7. The amount of bound substrate after each incubation time with cold competitor is expressed as a percentage of the total bound substrate at time zero (no incubation with competitor) and shown on the *y* axis.

TABLE 1. K_d values of AID to DNA substrates[a]

Substrate	GST-AID K_d (nM)	His-AID K_d (nM)
HS5ss	3.33 ± 1.27 1.40 ± 0.80[b]	9.73 ± 2.68
CS5ss	1.19 ± 0.21 1.90 ± 0.80[b]	8.21 ± 2.80
HS1bub5	1.06 ± 0.24	ND
HS1bub7	0.28 ± 0.07	2.15 ± 1.00
HS1bub11	0.46 ± 0.15	ND
HS3bub7	0.32 ± 0.11	ND
CS1bub7	ND	0.97 ± 0.25
CS3bub7	0.29 ± 0.11	ND

[a] All values obtained using UV-cross-linked data from EMSA gels, unless otherwise indicated. ND, not determined.
[b] Determined by NECEEM.

the results shown in Fig. 4D, we determined the half-life of GST-AID on HS1bub7 to be approximately 8 min, indicative of relatively high complex stability.

AID complex formation on ssDNA. As the WRC and non-WRC motifs constitute only a small fraction of the entire single-stranded region of the bubble, it remained plausible that binding differences to such motifs cannot be discerned in the context of the other single-stranded sequences within the bubble. Thus, we measured AID binding to single-stranded oligonucleotides HS5ss and CS5ss by EMSA, each bearing multiple tandem hot or cold spots, respectively. As shown in Fig. 5A and B, GST-AID formed specific complexes with HS5ss and CS5ss, while GST did not (Fig. 5A and B, − lanes). This was also the case for His-AID (data not shown). As with the bubble sub-

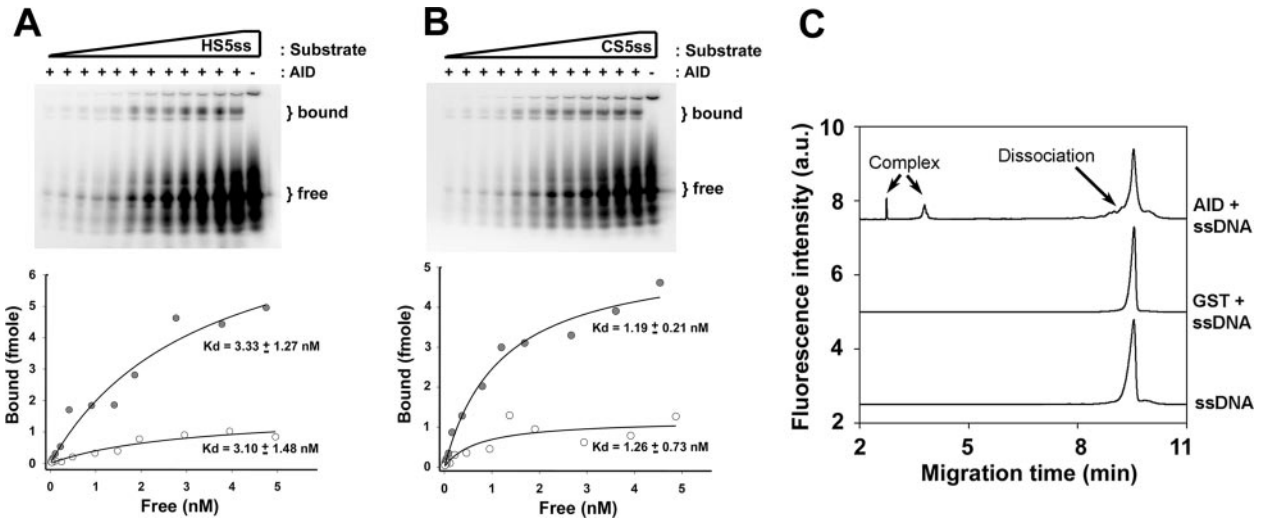

FIG. 5. Analysis of AID binding to single-stranded substrates. (A) Upper panel shows a representative native gel of an EMSA over a range of substrate concentrations of the HS5ss substrate (0.15 to 0.50 fmol) using GST (−) or GST-AID (+). The gel shown represents an EMSA experiment with UV cross-linking. In order to obtain half-saturation (K_d) values of interaction, the fraction of shifted substrate was quantitated for each lane, and a bound-versus-free plot was generated, as shown. Filled circles indicate the plot generated from the UV cross-linked EMSA experiment (gel shown), and open circles indicate the plot generated from the non-cross-linked EMSA experiment (gel not shown). (B) The same experiment as shown in panel A except that CS5ss was used as the substrate. (C) NECEEM analysis of AID-substrate dissociation showing the following superimposed NECEEM electropherograms (from top to bottom): 100 nM ssDNA plus 3 μM GST-AID, 100 nM ssDNA plus 20 μM GST, and 100 nM ssDNA. For a detailed description of NECEEM analysis, see Materials and Methods.

strates, higher levels of bound complex were observed with UV cross-linking, and the dissociation constants were similar between HS5ss and CS5ss with UV cross-linking, ranging between 1 and 3 nM (Fig. 5A and B and Table 1) for GST-AID and 8 and 10 nM for His-AID (Table 1). For both GST-AID and His-AID, these values were 3- to 10-fold higher than the K_d values measured on the bubble substrates (Table 1). Thus, AID has slightly lower binding affinities to single-stranded substrates than to bubble substrates.

We also determined dissociation constants between AID and HS5ss or CS5ss using the recently introduced NECEEM technique. NECEEM has been used for measuring equilibrium and kinetic parameters of protein-DNA interactions (3). This method is based on kinetic capillary electrophoresis, defined as capillary electrophoresis of species which interact under non-equilibrium conditions during electrophoresis (30). Binding reactions were carried out as in EMSA, except that the substrates were fluorescently labeled. A plug of the equilibrium mixture was injected into the capillary and allowed to dissociate during separation, resulting in characteristic peaks and dissociation curves in the electropherogram. Equilibrium constants and rate constants of complex dissociation can then be calculated by integrating the area under each peak of the electropherogram (see Materials and Methods for a detailed description of calculations).

As shown in Fig. 5C, binding to DNA is AID specific, since the GST control did not bind to DNA, even when GST was used at a concentration approximately 10-fold higher than AID-GST. As with the EMSA experiments, multiple complexes of AID-GST with DNA were observed (Fig. 5C) which likely correspond to complexes with different binding stoichiometries. We used the active concentration of the enzyme instead of the formal concentration in our determination of binding parameters by the NECEEM method (see Materials and Methods). As shown in Table 1, the K_d values between AID and hot-and cold-spot substrates were similar to each other (i.e., 1.4 and 1.9 nM, respectively), supporting the notion that AID binds to hot spots and cold spots with similar affinities. Furthermore, these K_d values were in good agreement with those measured by classical EMSA (Table 1).

In addition to measuring K_d values, we used the NECEEM to measure the rate constants of complex dissociation (i.e., k_{off}). The k_{off} values for HS5ss and CS5ss were $(1.8 \pm 0.3) \times 10^{-3}$ and $(2.8 \pm 1.1) \times 10^{-3}$, respectively. The half-life of complex dissociation [calculated using the equation $\ln(2)/k_{off}$] of AID-HS5ss and AID-CS5ss was 6.4 min and 4.1 min, respectively. Importantly, these results are in agreement with the 8-min half-life of GST-AID measured on HS1bub7 by EMSA. The rate constants of complex formation were also calculated as $k_{on} = k_{off}/K_d$. For both HS5ss and CS5ss, the k_{on} were 1.3×10^6 and 1.5×10^6 $M^{-1}s^{-1}$, which are similar to k_{on} values of other DNA binding proteins such as single-stranded binding protein (30). Thus, NECEEM confirmed the results by EMSA, namely, that there is no appreciable difference in the complex formation properties of AID on single-stranded substrates bearing tandem hot- or cold-spot motifs. Confirming the EMSA results obtained with the bubble-type substrates, the presence of cytidine on a single-stranded substrate was not required as measured by NECEEM to form complexes with AID (data not shown).

Deamination inhibition by hot- and cold-spot DNA substrates. The observation that AID can bind hot- and cold-spot bubbles with similar efficiency as measured by EMSA and NECEEM predicts that hot- and cold-spot bubble competitors should be able to inhibit the enzymatic activity of AID to similar degrees. To test this, we used several hot- and cold-spot

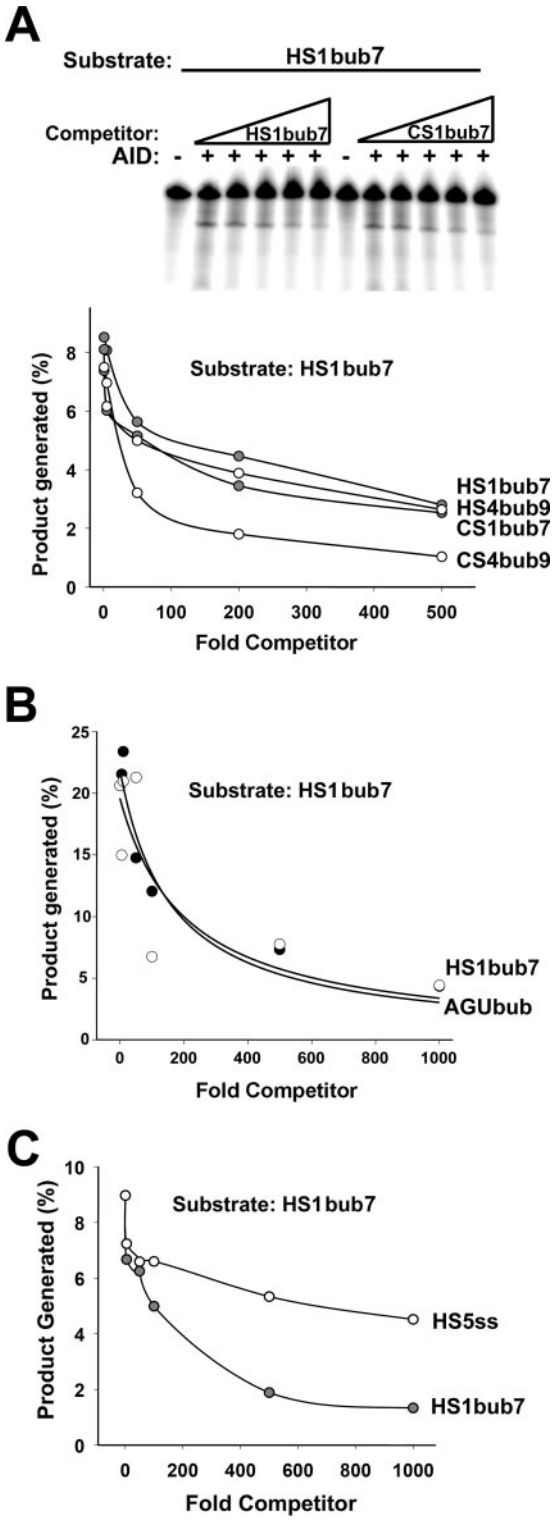

FIG. 6. Deamination inhibition by hot- and cold-spot competitors. (A) Upper panel shows a representative deamination assay using GST (−) or GST-AID (+) with 50 fmol of HS1bub7 as substrate. Reactions were carried out in the presence of increasing amounts (5- to 500-fold) of excess unlabeled hot-spot bubble competitor (HS1bub7) or cold-spot bubble competitor (CS1bub7) which were added to the reaction mixture before the addition of AID. Additional deamination inhibition assays were performed using HS1bub7 as the substrate and excess unlabeled HS1bub7, HS4bub9, CS1bub7, and CS4bub9 as cold competitors (gels not shown), and the results are shown in the graph. For each lane, the amount of cleavage product was quantitated and expressed as a percentage of total substrate. This value is shown on the *y* axis as a function of the increasing amounts of unlabeled competitor on the *x* axis. (B) Graphs are as described for panel A, except that 20 fmol of HS1bub7 was used as the substrate and unlabeled HS1bub7 and AGUbub were used as excess unlabeled competitors (5- to 1,000-fold excess). (C) Graphs are as described for panel A, except that HS1bub7 and HS5ss were used as excess unlabeled competitors (5- to 1,000-fold excess).

bubbles as unlabeled competitors in the deamination assay. We measured the inhibition of AID activity on HS1bub7 in the presence of excess unlabeled hot-spot bubble competitors (HS1bub7 and HS4bub) as well as two unlabeled cold-spot bubble competitors (CS1bub7 and CS4bub). A typical assay is shown in Fig. 6A (top). As shown in Fig. 6A (bottom), the capacities of all four unlabeled hot- and cold-spot bubbles to inhibit deamination were comparable. This further supports the notion that AID binds to hot-spot and cold-spot bubbles with similar affinities. Furthermore, as GST-AID binding did not require the presence of a cytidine in the bubble region of the substrates (see above), we tested whether a cytidine was required for the inhibition of AID activity. As shown in Fig. 6B, when used as unlabeled competitor, AGUbub was equally proficient at inhibiting deamination activity as HS1bub7. Thus, any excess bubble substrate, whether it contains one, multiple, or no cytidines, is able to bind and sequester AID, thereby inhibiting its activity on the labeled substrate.

AID seemed to bind with higher affinities to the bubble substrates bearing one hot spot or cold spot than to the single-stranded substrates bearing tandem hot and cold spots (see above). To further corroborate this result, we tested HS5ss and HS1bub7 as excess unlabeled competitors in an enzymatic activity assay on HS1bub7. As shown in Fig. 6C, excess HS1bub7 inhibited the enzymatic activity of AID better than HS5ss. Taken together, the reduced ability of HS5ss to inhibit the enzymatic activity of AID and the higher K_d values for binding to single-stranded substrates than to bubble substrates indicate that AID preferentially binds to a restricted bubble DNA structure rather than a more flexible ssDNA substrate.

Stoichiometry of active GST-AID. Relative to the DNA substrates used in the deamination and EMSA experiments, a molar excess of both GST-AID and His-AID protein had to be used to detect appreciable enzymatic activity as well as complex formation. This suggested that, much like other mammalian proteins expressed in bacteria, only a fraction of the preparation exists in an active form. This notion was supported by our calculation of the active fraction of GST-AID using $\text{Bound}_{\text{max}}$ values in the EMSA experiments as described above. In addition, EMSA with both GST-AID and His-AID revealed multiple complexes with different mobilities, indicative of various stoichiometric proportions of AID relative to the DNA substrates. Together, these data suggested that the AID preparations likely exist as a heterogenous mixture of active and inactive AID as well as in different multimeric forms. To gain insight into this, we used size-exclusion chromatography by FPLC to separate a GST-AID preparation and assay each fraction for activity. Molecular mass standards were

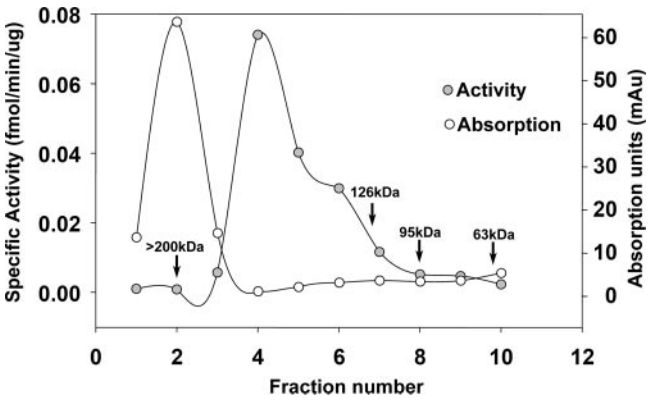

FIG. 7. FPLC analysis of GST-AID. GST-AID was fractionated using a 200-kDa size exclusion column on an automated FPLC machine. Fractions were eluted, and each fraction was tested in the deamination assay. The curve with open circles shows the UV absorption value for each fraction as it was eluted from the column, thus representing the amount of GST-AID in each fraction. The curve with filled circles represents the results of the deamination assay on each fraction. Briefly, fractions were concentrated and incubated with 20 fmol of HS1bub7 substrate and UDG in an activity buffer. The amount of cleaved product was quantitated and divided by the reaction incubation time and the amount of input GST-AID (calculated from the UV absorption values) to obtain the specific activity of each fraction. Arrows indicate elution points of molecular mass standards on the same column, allowing for the estimation of the molecular mass of each GST-AID species in each fraction.

separated on the same column (Fig. 7, arrows). Figure 7 shows a chromatogram of the FPLC separation overlaid on a curve of specific deamination activity of each fraction as determined by the UDG assay. As apparent in the chromatogram in Fig. 7, the largest peak of the GST-AID preparation was greater than 200 kDa, indicating that the majority of the preparation was aggregated. The fractions with the highest specific activity fell in the range of the dimer-tetramer of GST-AID (Fig. 7), while the fraction containing GST-AID monomers (molecular mass of 53 kDa) exhibited no appreciable activity. These data are consistent with a recent finding showing that AID exists as a dimer in cells (51). Interestingly, the fractions with the highest specific activity (fractions 4 to 6), which represented a small fraction of the entire preparation, did not have higher specific activities than previous assays that used unfractionated GST-AID (Fig. 3A). This suggests that the dimer-tetramer fractions of AID were reaggregating after purification. Indeed, this was confirmed by FPLC analysis (data not shown).

DISCUSSION

In this report, we examined the biochemical basis for the selective deamination of WRC motifs by AID. One possible explanation for this property of AID is that AID has a higher binding affinity for WRC motifs than for other motifs. However, using different approaches, we found that this was not the case. First, the apparent dissociation constants of AID for single-stranded or bubble hot-spot or cold-spot substrates were similar, regardless of the assay used (i.e., EMSA or NECEEM) (Fig. 4 and 5). Second, unlabeled hot- or cold-spot competitors were equally efficient at inhibiting AID activity, indicating that hot- and cold-spot substrates can similarly secure AID binding. Thus, AID in its entirety is a sequence-independent ssDNA binding protein that does not even require a cytidine to bind ssDNA. In this regard, our finding provides an explanation for the suggested processive-like trait of AID on ssDNA (31) by allowing for a "scanning" mode of WRC capture. This type of activity has also been reported for restriction enzymes such as EcoRI (53). The precise mechanism of how the active site of AID may recognize the dinucleotide upstream of its target will form the basis for future studies.

The calculated K_d of AID for bubble substrates was in the 0.3 to 2 nM range, which indicates that AID binds bubble substrates with high affinity, similar to that of other DNA-binding proteins. For example, single-stranded binding protein has a K_d of ~1 to 10 nM (30), while some transcription factors have subnanomolar K_d values (e.g., transcription factor IIIA has a K_d of 0.1 nM) (41). Because enzymes typically have K_ds in the micromolar range, the finding that AID binds to substrates in the nanomolar range, has a long half-life of complex dissociation of 4 to 8 min on ssDNA and bubble substrates (see above), and is sequence independent would predict that AID has a low catalytic efficiency since it would remain bound after deamination. Indeed, we calculated that each molecule of AID catalyzes a deamination once every 4 min (see above), which makes AID a very poor enzyme since many enzymes can usually catalyze hundreds to thousands of reactions per second. This finding is significant since it would imply that after a deamination event, AID might reside for long periods of time on immunoglobulin sequences and possibly act as a scaffolding protein to recruit other DNA repair factors. Findings that AID can associate with proteins such as RPA (7) and MDM2 (19) support this notion.

Competition experiments (Fig. 6) and the higher K_d values calculated for ssDNA substrates versus bubble substrates for both GST-AID and His-AID indicate that AID may prefer a more rigid bubble substrate than the flexible ssDNA substrates. This is particularly emphasized by the fact that each ssDNA substrate has more single-stranded nucleotides than a bubble substrate and should therefore be able to bind more AID than the bubble substrate. This finding provides an explanation for a previous observation (6) that AID preferentially deaminates cytidines within bubble substrates and is consistent with its primary targets' residing within transcription bubbles. However, while typical transcription bubbles are thought to be 14 to 17 nucleotides in size (48), GST-AID preferably deaminated targets located within 5- and 7-nucleotide bubbles compared to longer bubbles of up to 17 nucleotides. These results are in contrast to a previous finding where a 9-nucleotide bubble was a more efficient target than its 5-nucleotide counterpart (6). This discrepancy might be due to differences in the local sequence within the bubbles, as has been shown before (54). The significance of this preference of AID for smaller bubbles than for typical transcription bubbles is unclear. One possibility is that the transcription bubble accessible by AID is smaller than 14 to 17 nucleotides due to partial coverage by the RNA polymerase complex and that AID has evolved to be optimally active in the context of the accessible portion of the bubble. However, questions have been raised regarding the model that AID acts on transcription bubbles with findings that AID mutates both strands equally, despite the protection offered by the nascent transcript to the

template strand. In this light, an alternative explanation is that AID may preferentially act on stem-loop bubble structures which are smaller in size than transcription bubbles and might be generated during the transcription or replication of DNA due to the local unwinding of DNA (16, 46). Whatever the case may be, we have shown here that the difference in AID activity on different-size bubbles is not due to substrate binding. Thus, it is tempting to speculate that the preferential activity of AID on smaller bubbles might reflect an active site that better accommodates smaller bubbles or that smaller bubbles are better able to induce a conformational change in AID that is required for the subsequent deamination reaction.

The fact that 4 fmol of AID was active in our assays indicates that a large fraction of AID was inactive (see Materials and Methods). This issue along with the presence of multiple shifted bands with GST-AID and His-AID prompted us to examine the composition of our in vitro-purified AID preparations. Using FPLC analysis, we showed that the majority of our AID preparations exist as aggregates with low specific activity, while a small portion of soluble AID containing AID tetramers and dimers exhibits high enzymatic activity. These data support the recent finding that AID exists as a dimer in cells (51). The finding that our purified AID is largely inactive is also likely to be the case for other studies that examined AID which used picomole quantities of AID and femtomole quantities of substrate (5, 6, 10, 45, 47, 54) and is, indeed, the case for other delicate enzymes such as Rag 1 and 2 (14, 35). The difficulty with in vitro studies of such enzymes, including AID, lies with their poor solubility properties, suggesting that other factors in the cellular environment act to stabilize them. Indeed, we observed by FPLC that the most active oligomeric AID can reaggregate into larger but less active complexes upon purification. It is important to note that the tendency of in vitro-purified AID to form aggregates may not reflect the in vivo state, where its copy number in each cell is tightly regulated and where it may form complexes with other protein factors.

A distinction between bacterially expressed AID and that expressed in eukaryotic cells may lie in differences in posttranslational modifications such as phosphorylation. Though it has been shown that phosphorylation of AID by protein kinase A at serine 38 upregulates its activity (2, 24), the precise role of this modification remains unknown, as a recent report suggests that phosphorylation does not affect transcription-dependent deamination by AID with or without RPA in the reaction (4). Resolving these issues and developing a better understanding of the precise catalytic mechanism of AID require further work.

ACKNOWLEDGMENTS

We are grateful to David Isenman, Jacqueline Segall, and Marc Shulman for helpful discussions.

This research is supported by a grant from the Natural Sciences and Engineering Council to S.K. and a grant from the Canadian Institute of Health Research (MOP66965) to A.M. Both S.K. and A.M. are supported by Canada Research Chair awards. M.L. is supported by the David Rae memorial award from The Leukemia and Lymphoma Society of Canada.

REFERENCES

1. **Bachl, J., C. Carlson, V. Gray-Schopfer, M. Dessing, and C. Olsson.** 2001. Increased transcription levels induce higher mutation rates in a hypermutating cell line. J. Immunol. **166:**5051–5057.
2. **Basu, U., J. Chaudhuri, C. Alpert, S. Dutt, S. Ranganath, G. Li, J. P. Schrum, J. P. Manis, and F. W. Alt.** 2005. The AID antibody diversification enzyme is regulated by protein kinase A phosphorylation. Nature **438:**508–511.
3. **Berezovski, M., and S. N. Krylov.** 2002. Non-equilibrium capillary electrophoresis of equilibrium mixtures–a single experiment reveals equilibrium and kinetic parameters of protein-DNA interactions. J. Am. Chem. Soc. **124:**13674–13675.
4. **Besmer, E., E. Market, and F. N. Papavasiliou.** 2006. The transcription elongation complex directs activation-induced cytidine deaminase-mediated DNA deamination. Mol. Cell. Biol. **26:**4378–4385.
5. **Bransteitter, R., P. Pham, P. Calabrese, and M. F. Goodman.** 2004. Biochemical analysis of hypermutational targeting by wild type and mutant activation-induced cytidine deaminase. J. Biol. Chem. **279:**51612–51621.
6. **Bransteitter, R., P. Pham, M. D. Scharff, and M. F. Goodman.** 2003. Activation-induced cytidine deaminase deaminates deoxycytidine on single-stranded DNA but requires the action of RNase. Proc. Natl. Acad. Sci. USA **100:**4102–4107.
7. **Chaudhuri, J., C. Khuong, and F. W. Alt.** 2004. Replication protein A interacts with AID to promote deamination of somatic hypermutation targets. Nature **430:**992–998.
8. **Chaudhuri, J., M. Tian, C. Khuong, K. Chua, E. Pinaud, and F. W. Alt.** 2003. Transcription-targeted DNA deamination by the AID antibody diversification enzyme. Nature **422:**726–730.
9. **Chen, X., K. Kinoshita, and T. Honjo.** 2001. Variable deletion and duplication at recombination junction ends: implication for staggered double-strand cleavage in class-switch recombination. Proc. Natl. Acad. Sci. USA **98:**13860–13865.
10. **Dickerson, S. K., E. Market, E. Besmer, and F. N. Papavasiliou.** 2003. AID mediates hypermutation by deaminating single-stranded DNA. J. Exp. Med. **197:**1291–1296.
11. **Duquette, M. L., P. Handa, J. A. Vincent, A. F. Taylor, and N. Maizels.** 2004. Intracellular transcription of G-rich DNAs induces formation of G-loops, novel structures containing G4 DNA. Genes Dev. **18:**1618–1629.
12. **Duquette, M. L., P. Pham, M. F. Goodman, and N. Maizels.** 2005. AID binds to transcription-induced structures in c-MYC that map to regions associated with translocation and hypermutation. Oncogene **24:**5791–5798.
13. **Franco, S., M. Gostissa, S. Zha, D. B. Lombard, M. M. Murphy, A. A. Zarrin, C. Yan, S. Tepsuporn, J. C. Morales, M. M. Adams, Z. Lou, C. H. Bassing, J. P. Manis, J. Chen, P. B. Carpenter, and F. W. Alt.** 2006. H2AX prevents DNA breaks from progressing to chromosome breaks and translocations. Mol. Cell **21:**201–214.
14. **Fugmann, S. D., I. J. Villey, L. M. Ptaszek, and D. G. Schatz.** 2000. Identification of two catalytic residues in RAG1 that define a single active site within the RAG1/RAG2 protein complex. Mol. Cell **5:**97–107.
15. **Huang, F. T., K. Yu, C. L. Hsieh, and M. R. Lieber.** 2006. Downstream boundary of chromosomal R-loops at murine switch regions: implications for the mechanism of class switch recombination. Proc. Natl. Acad. Sci. USA **103:**5030–5035.
16. **Kinoshita, K., and T. Honjo.** 2001. Linking class-switch recombination with somatic hypermutation. Nat. Rev. Mol. Cell Biol. **2:**493–503.
17. **Larijani, M., D. Frieder, W. Basit, and A. Martin.** 2005. The mutation spectrum of purified AID is similar to the mutability index in Ramos cells and in ung(−/−) msh2(−/−) mice. Immunogenetics **56:**840–845.
18. **Larijani, M., D. Frieder, T. M. Sonbuchner, R. Bransteitter, M. F. Goodman, E. E. Bouhassira, M. D. Scharff, and A. Martin.** 2005. Methylation protects cytidines from AID-mediated deamination. Mol. Immunol. **42:**599–604.
19. **Macduff, D. A., M. S. Neuberger, and R. S. Harris.** 2005. MDM2 can interact with the C terminus of AID but it is inessential for antibody diversification in DT40 B cells. Mol. Immunol. **43:**1099–1108.
20. **Martin, A., P. D. Bardwell, C. J. Woo, M. Fan, M. J. Shulman, and M. D. Scharff.** 2002. Activation-induced cytidine deaminase turns on somatic hypermutation in hybridomas. Nature **415:**802–806.
21. **Martin, A., Z. Li, D. P. Lin, P. D. Bardwell, M. D. Iglesias-Ussel, W. Edelmann, and M. D. Scharff.** 2003. Msh2 ATPase activity is essential for somatic hypermutation at A-T basepairs and for efficient class switch recombination. J. Exp. Med. **198:**1171–1178.
22. **Martin, A., and M. D. Scharff.** 2002. AID and mismatch repair in antibody diversification. Nature Rev. Immunol. **2:**605–614.
23. **Martomo, S. A., D. Fu, W. W. Yang, N. S. Joshi, and P. J. Gearhart.** 2005. Deoxyuridine is generated preferentially in the nontranscribed strand of DNA from cells expressing activation-induced cytidine deaminase. J. Immunol. **174:**7787–7791.
24. **McBride, K. M., A. Gazumyan, E. M. Woo, V. M. Barreto, D. F. Robbiani, B. T. Chait, and M. C. Nussenzweig.** 2006. Regulation of hypermutation by activation-induced cytidine deaminase phosphorylation. Proc. Natl. Acad. Sci. USA **103:**8798–8803.

25. **Morgan, H. D., W. Dean, H. A. Coker, W. Reik, and S. K. Petersen-Mahrt.** 2004. Activation-induced cytidine deaminase deaminates 5-methylcytosine in DNA and is expressed in pluripotent tissues: implications for epigenetic reprogramming. J. Biol. Chem. **279:**52353–52360.
26. **Muramatsu, M., K. Kinoshita, S. Fagarasan, S. Yamada, Y. Shinkai, and T. Honjo.** 2000. Class switch recombination and hypermutation require activation-induced cytidine deaminase (AID), a potential RNA editing enzyme. Cell **102:**553–563.
27. **Pasqualucci, L., Y. Kitaura, H. Gu, and R. Dalla-Favera.** 2006. PKA-mediated phosphorylation regulates the function of activation-induced deaminase (AID) in B cells. Proc. Natl. Acad. Sci. USA **103:**395–400.
28. **Peters, A., and U. Storb.** 1996. Somatic hypermutation of immunoglobulin genes is linked to transcription initiation. Immunity **4:**57–65.
29. **Petersen-Mahrt, S. K., R. S. Harris, and M. S. Neuberger.** 2002. AID mutates *E. coli* suggesting a DNA deamination mechanism for antibody diversification. Nature **418:**99–104.
30. **Petrov, A., V. Okhonin, M. Berezovski, and S. N. Krylov.** 2005. Kinetic capillary electrophoresis (KCE): a conceptual platform for kinetic homogeneous affinity methods. J. Am. Chem. Soc. **127:**17104–17110.
31. **Pham, P., R. Bransteitter, J. Petruska, and M. F. Goodman.** 2003. Processive AID-catalysed cytosine deamination on single-stranded DNA simulates somatic hypermutation. Nature **424:**103–107.
32. **Price, N. C., and L. Stevens.** 1999. Fundamentals of enzymology: the cell and molecular biology of catalytic proteins, 3rd ed. Oxford University Press, Oxford, United Kingdom.
33. **Rada, C., J. M. Di Noia, and M. S. Neuberger.** 2004. Mismatch recognition and uracil excision provide complementary paths to both Ig switching and the A/T-focused phase of somatic mutation. Mol. Cell **16:**163–171.
34. **Rada, C., G. T. Williams, H. Nilsen, D. E. Barnes, T. Lindahl, and M. S. Neuberger.** 2002. Immunoglobulin isotype switching is inhibited and somatic hypermutation perturbed in UNG-deficient mice. Curr. Biol. **12:**1748–1755.
35. **Raghavan, S. C., P. C. Swanson, Y. Ma, and M. R. Lieber.** 2005. Double-strand break formation by the RAG complex at the bcl-2 major breakpoint region and at other non-B DNA structures in vitro. Mol. Cell. Biol. **25:**5904–5919.
36. **Ramiro, A. R., M. Jankovic, E. Callen, S. Difilippantonio, H. T. Chen, K. M. McBride, T. R. Eisenreich, J. Chen, R. A. Dickins, S. W. Lowe, A. Nussenzweig, and M. C. Nussenzweig.** 2006. Role of genomic instability and p53 in AID-induced c-myc-Igh translocations. Nature **440:**105–109.
37. **Ramiro, A. R., M. Jankovic, T. Eisenreich, S. Difilippantonio, S. Chen-Kiang, M. Muramatsu, T. Honjo, A. Nussenzweig, and M. C. Nussenzweig.** 2004. AID is required for c-myc/IgH chromosome translocations in vivo. Cell **118:**431–438.
38. **Ramiro, A. R., P. Stavropoulos, M. Jankovic, and M. C. Nussenzweig.** 2003. Transcription enhances AID-mediated cytidine deamination by exposing single-stranded DNA on the nontemplate strand. Nat. Immunol. **4:**452–456.
39. **Rogozin, I. B., and M. Diaz.** 2004. Cutting edge: DGYW/WRCH is a better predictor of mutability at G:C bases in Ig hypermutation than the widely accepted RGYW/WRCY motif and probably reflects a two-step activation-induced cytidine deaminase-triggered process. J. Immunol. **172:**3382–3384.
40. **Rogozin, I. B., and N. A. Kolchanov.** 1992. Somatic hypermutagenesis in immunoglobulin genes. II. Influence of neighbouring base sequences on mutagenesis. Biochim. Biophys. Acta **1171:**11–18.
41. **Rowland, O., and J. Segall.** 1996. Interaction of wild-type and truncated forms of transcription factor IIIA from *Saccharomyces cerevisiae* with the 5S RNA gene. J. Biol. Chem. **271:**12103–12110.
42. **Rush, J. S., S. D. Fugmann, and D. G. Schatz.** 2004. Staggered AID-dependent DNA double strand breaks are the predominant DNA lesions targeted to Sμ in Ig class switch recombination. Int. Immunol. **16:**549–557.
43. **Schrader, C. E., E. K. Linehan, S. N. Mochegova, R. T. Woodland, and J. Stavnezer.** 2005. Inducible DNA breaks in Ig S regions are dependent on AID and UNG. J. Exp. Med. **202:**561–568.
44. **Shapiro, G. S., K. Aviszus, J. Murphy, and L. J. Wysocki.** 2002. Evolution of Ig DNA sequence to target specific base positions within codons for somatic hypermutation. J. Immunol. **168:**2302–2306.
45. **Shen, H. M., S. Ratnam, and U. Storb.** 2005. Targeting of the activation-induced cytosine deaminase is strongly influenced by the sequence and structure of the targeted DNA. Mol. Cell. Biol. **25:**10815–10821.
46. **Shen, H. M., and U. Storb.** 2004. Activation-induced cytidine deaminase (AID) can target both DNA strands when the DNA is supercoiled. Proc. Natl. Acad. Sci. USA **101:**12997–13002.
47. **Sohail, A., J. Klapacz, M. Samaranayake, A. Ullah, and A. S. Bhagwat.** 2003. Human activation-induced cytidine deaminase causes transcription-dependent, strand-biased C to U deaminations. Nucleic Acids Res. **31:**2990–2994.
48. **Spitalny, P., and M. Thomm.** 2003. Analysis of the open region and of DNA-protein contacts of archaeal RNA polymerase transcription complexes during transition from initiation to elongation. J. Biol. Chem. **278:**30497–30505.
49. **Suelter, C. H.** 1985. A practical guide to enzymology. John Wiley & Sons, Hoboken, NJ.
50. **Wakae, K., B. G. Magor, H. Saunders, H. Nagaoka, A. Kawamura, K. Kinoshita, T. Honjo, and M. Muramatsu.** 15 November 2005, posting date. Evolution of class switch recombination function in fish activation-induced cytidine deaminase, AID. Int. Immunol. doi:10.1093/intimm/dxh347.
51. **Wang, J., R. Shinkura, M. Muramatsu, H. Nagaoka, K. Kinoshita, and T. Honjo.** 2006. Identification of a specific domain required for dimerization of activation-induced cytidine deaminase. J. Biol. Chem. **281:**19115–19123.
52. **Wilson, T. M., A. Vaisman, S. A. Martomo, P. Sullivan, L. Lan, F. Hanaoka, A. Yasui, R. Woodgate, and P. J. Gearhart.** 2005. MSH2-MSH6 stimulates DNA polymerase eta, suggesting a role for A:T mutations in antibody genes. J. Exp. Med. **201:**637–645.
53. **Woodhead, J. L., and A. D. Malcolm.** 1980. Non-specific binding of restriction endonuclease EcoRI to DNA. Nucleic Acids Res. **8:**389–402.
54. **Yu, K., F. T. Huang, and M. R. Lieber.** 2004. DNA substrate length and surrounding sequence affect the activation-induced deaminase activity at cytidine. J. Biol. Chem. **279:**6496–6500.
55. **Zarrin, A. A., F. W. Alt, J. Chaudhuri, N. Stokes, D. Kaushal, L. Du Pasquier, and M. Tian.** 2004. An evolutionarily conserved target motif for immunoglobulin class-switch recombination. Nat. Immunol. **5:**1275–1281.
56. **Zhang, W., P. D. Bardwell, C. J. Woo, V. Poltoratsky, M. D. Scharff, and A. Martin.** 2001. Clonal instability of V region hypermutation in the Ramos Burkitt's lymphoma cell line. Int. Immunol. **13:**1175–1184.